

Caroline Bedin

PID Detection in Crystalline Silicon Modules Using Low-Cost Electroluminescence Images in the Field

Caroline Bedin¹, Aline Kirsten Vidal de Oliveira¹, Lucas Rafael do Nascimento¹, Gustavo Xavier de Andrade Pinto¹, Lucas Augusto Zanicoski Sergio¹ and Ricardo R  ther¹

¹*Universidade Federal de Santa Catarina, Florian  polis–SC, 88040-900, Brazil*
www.fotovoltaica.ufsc.br
E-mail: carolinebed@gmail.com

Abstract

Assessing the state of integrity of photovoltaic (PV) modules using the electroluminescence (EL) method was predominantly carried out by manufacturers to evaluate the quality of their production line. Nowadays, conventional cameras can be adapted to perform laboratory tests and by adjusting a few conditions, it is possible to carry out these tests in the field. The present study analyses the detection of Potential Induced Degradation (PID) in multicrystalline silicon PV modules installed and operating at a test site in the city of Capivari de Baixo, located in the Southern region of Brazil (Lat: -28.4398, Lon: -48.9575), applying a modified low-cost camera. The pattern in the images of the modules affected by PID is very clear, allowing an accurate detection through the electroluminescence images. However, in order to quantify the level of degradation, some electrical parameters can be analysed, such as the modules parallel resistance, open circuit voltage and short circuit current. To obtain the electrical parameters, the current-voltage curves (IV-curve) of the modules were measured, proving the efficiency of PID detection using low-cost EL images obtained in the field.

1. Introduction

In recent years, there has been a significant increase in PV installations in sunbelt countries, with Australia and Brazil presenting increases of 23% and 1,000% in PV installed capacity, respectively, from 2016 to 2017 (IRENA, 2018). With the increased number of installed PV systems, the reliability and durability assessment of this technology becomes essential, as crystalline silicon-based PV is subject to PID, especially in high-voltage, utility-scale applications (Mart  nez-Moreno et al., 2018).

PID is easily detected through IV-curve measurements or EL images. The EL phenomenon is revealed when an electric current is injected into the active circuit of a PV cell, causing it to emit radiation. Loss of this property indicates that the affected portion will no longer be contributing to the PV effect. Typical commercial solutions include high-cost and high-performance cameras. However, conventional digital cameras can be adapted to capture EL images allowing the detection of nonidealities in PV modules at a significantly lower cost (IEA-PVPS, 2018). This work aims at analysing the application of a low-cost method based on EL images, in order to detect PID in PV systems and validate the images with electrical parameter measurements.

2. Overview

The voltage difference between frame and cell of a PV module, associated with high temperature and humidity conditions, can cause sodium ions (Na^+) to migrate from the front glass to the junction of the cell. This accumulation of ions will cause the parallel resistance of the module to decrease and consequently the leakage current to the ground is increased, characterizing PID (Colli, et al 2013 and Naumann, et al 2014). The degradation will cause other parameters of the modules to be affected, such as maximum power point and open circuit voltage. The PID effect will be larger in the most negative part of photovoltaic arrays exposed to high voltages in normal operation (Oh et al., 2017). Figure 1 represents the IV-curve of a healthy module (in blue) and a module affected by PID (in red).

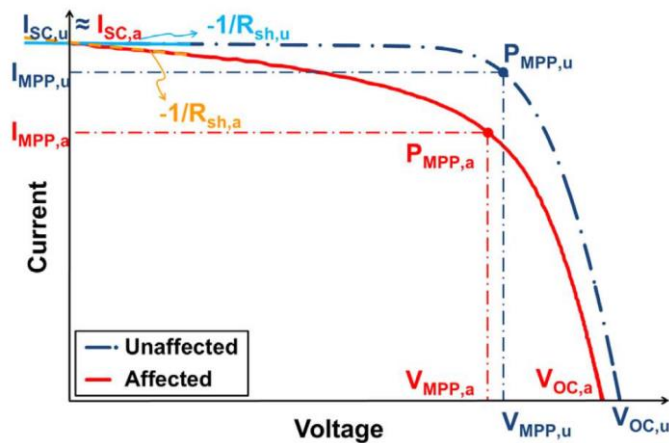


Figure 1. IV curve of a PV module unaffected (dashed blue line) and affected by PID (continuous red line). (Martínez-Moreno et al., 2018)

Through the shapes of the curves, it is possible to detect some parameters, such as: short-circuit current, I_{SC} , open circuit voltage, V_{OC} , series resistance, R_S , and shunt resistance, R_{SH} . Normal module operation is near the maximum power point (P_{MPP}) with corresponding current and voltage values (I_{MPP} and V_{MPP} , respectively). The decrease in shunt resistance translates into a greater slope of the IV curve near the short circuit area. The PID will cause the parameters of the IV-curve to change with a characteristic pattern. The reduction of the R_{SH} results in lower values of the P_{PMM} , I_{PMM} and V_{PMM} , as seen in the red curve of Figure 1. (Martínez-Moreno et al., 2018).

EL is a non-invasive method for the detection of cell and module defects; EL images can be obtained from photons emitted by the radiative recombination of charge carriers excited under forward bias. An external power supply is used to electrically stimulate the module to emit electroluminescent radiation with a wavelength in the 1,150nm range. Cell defects locally reduce or prevent the emission of EL radiation and can be visualised as black areas by cameras that are sensitive to these wavelengths (Djordjevic, et al 2014 and Frazão, et al 2017). Nowadays, advanced commercial solutions are available in order to obtain these images. However, low cost solutions can be achieved by adapting conventional digital cameras, with the extraction of the infrared filter, allowing the visualization of the electroluminescent range of crystalline silicon. Figure 2 shows the range of emission spectra for crystalline silicon modules and the quantum efficiency of the camera sensor used to obtain EL images.

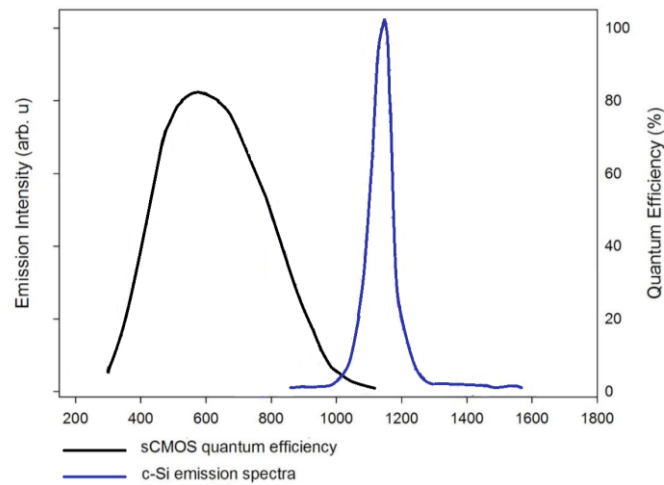


Figure 2. Emission spectra from a range of crystalline silicon solar cell and the quantum efficiency of sCMOS cameras (adapted from IEA-PVPS, 2018).

It can be observed that the wavelength of crystalline silicon peaks at 1,150nm. The silicon based sensor Complementary Metal Oxide Semiconductor (CMOS) used has a low quantum efficiency in the portion of wavelength along the spectrum of crystalline silicon. Although it seems impossible to perform EL imaging with this type of sensor, some measures are employed to make the EL test feasible, such as: removing the infrared filter and obtaining photos in dimly lit places such as after the sunset.

As shown in Figure 3, the EL images of multicrystalline silicon modules affected by PID present a pattern of darker cells at the edges of the modules, due to the shorter distance between these cells and the frame. The black parts represent the associated energy loss due to leakage current, a phenomenon that will increase with time and climatic conditions. Modules that are exposed to high temperatures and humidity will experience this strong effect (Luo et al., 2017).

The decrease of shunt resistance in a photovoltaic module will cause it to lose part or completely the electroluminescent property, depending on the degree of degradation of the cells. Several mechanisms of degradation may cause the module to lose this property. The PID can be easily differentiated from the other degradations because the cells near the edges will be darker than the middle ones, for reasons previously announced.

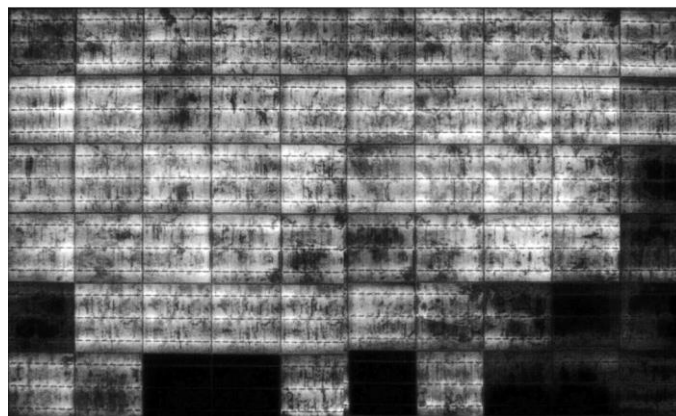


Figure 3. Module affected by PID, with a pattern of cells darker at the PV module edges.

3. Methodology

The experiment was carried out at a 9 kWp c-Si PV array operating at one of the eight test sites spread over the Brazilian territory. They were built by Fotovoltaica/UFSC together with *ENGIE Brasil Energia* in a R&D project in 2013, as is shown in Figure 4. The project aimed to assess the performance of seven different, commercially-available PV technologies: thin-film amorphous silicon (a-Si), microcrystalline silicon (a-Si/ μ c-Si), cadmium telluride (CdTe), copper indium gallium diselenide (CIGS), and both mono and multi-crystalline silicon (c-Si and m-Si), all at fixed and latitude tilt (Rüther et al., 2017; Nascimento et al., 2018). This experiment focused on the Capivari de Baixo test site, in the south of Santa Catarina (Lat: -28.4398, Lon: -48.9575) which is on a coastal area, with high relative temperatures and humidity.

The data of energy production of the evaluation sites are continuously stored and analysed since they came into operation. After observing an underperformance of the evaluation site of Capivari de Baixo over the years, some field measurements were carried out. The electrical measurements revealed a reduction of the open-circuit voltage of the modules and given the weather conditions of the coast region and the high susceptibility of this technology to suffer such degradation, the hypothesis of PID was raised. For verifying this suspicion, EL pictures were then taken after sunset and IV-curve measurements were performed under daylight confirming the diagnostic obtained with the EL tests.



Figure 4. Capivari de Baixo site and the eight identical PV technology test sites located at eight different climatic regions in Brazil.

A Sony Cyber-shot DSC-WX9 16.2 megapixel digital camera with a sCMOS sensor was used to obtain the EL images. The conventional camera was adapted by a professional, specialized in photographic cameras, which removed the infrared filter of the camera, allowing the visualization of the luminescence in the range of the crystalline silicon spectrum (IEA-PVPS, 2018). In order to validate the use of low-cost cameras, an EL image comparison was carried out with three other cameras (GoPro 3 Plus Black, Canon Rebel EOS T6i - EF-S 18-55 IS STM and Canon EOS M3 - PV vision EL Lent 1.4/50) where the infrared filters were removed. The comparison was performed in the laboratory, using a module diagnosed with PID. The pictures of each camera were taken under the same conditions.

For the validation of the field detection of PID, EL pictures were taken in the field after sunset, allowing the adapted camera to easily capture only the light emitted by the module and not from the surroundings. During the measurements, the camera was set to night mode, allowing less light to pass through the shutter, elongating the exposure time to capture the amount of light needed to take

the image. A voltage source was used to polarize four PV modules at a time with 55V and 9A (I_{sc}). Each module had its IV-curve measured individually in the next day under full sun.

Table 1 presents the results of the comparison between the low-cost camera and the other models. The pictures taken with each camera are followed by the price of acquisition of each model in Brazil, the table also show the additional modification cost by specialist for each camera. The camera 4 didn't need to have the filter removed, it was produced to capture EL images. For the comparison, a quotation of US\$ 1 = R\$ 4 was applied.

It is clear that the best results are obtained with camera 4. However, its weight, small angle of aperture and size make it unsuitable for on-site measurements. Its high price is given by the high cost of equipment customs duty. Camera 3 presented good results as well, showing dead cells, microcracks and even bad soldering problems in PV modules, however, this camera is more sensitive to the light of the environment and it becomes perceptible the light reflected in the metallic parts of the cells. Between the modified cameras, camera 2 showed the worst result. It could easily detect dead cells that are important for the detection of PID, but couldn't show small cracks on the cells, as Figure 5 (b) can show. Because of its low weight, small size and easy remote operation, it could be easily adapted to an Unmanned Aerial Vehicle (UAV) for a fast detection of PID in large-area, multi-megawatt PV power plants. Camera 1 present good results, given its price and size.

Figure 5 shows EL images obtained from a damaged cell with microcracks, where the higher efficiency of camera 4 (Figure 5(d)), the most expensive, is proven. Figure 5 confirms the results of the previous table, showing that camera 1 presents a good compromise between total equipment cost and image quality. Its image shows small uniformities of the material, dead fingers and microcracks, even more clear than the camera 3. Moreover, its low weight makes it easier to handle and use on tripods on site. These reasons led to the choice of camera 2 as the best alternative for the field detection of PID.

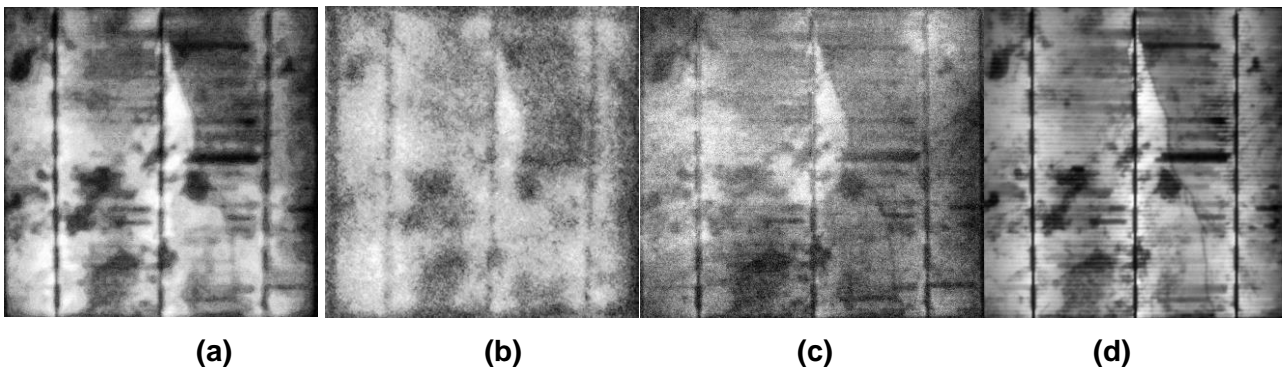

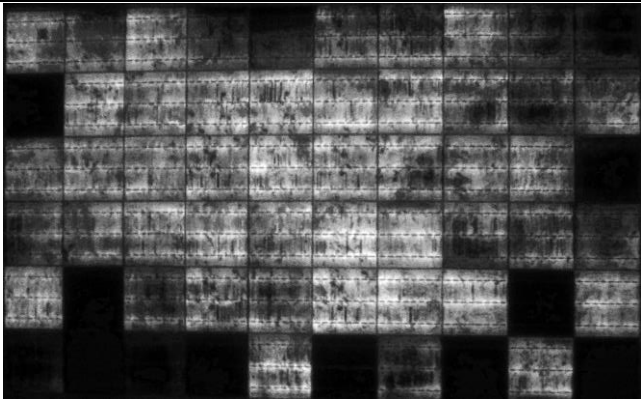

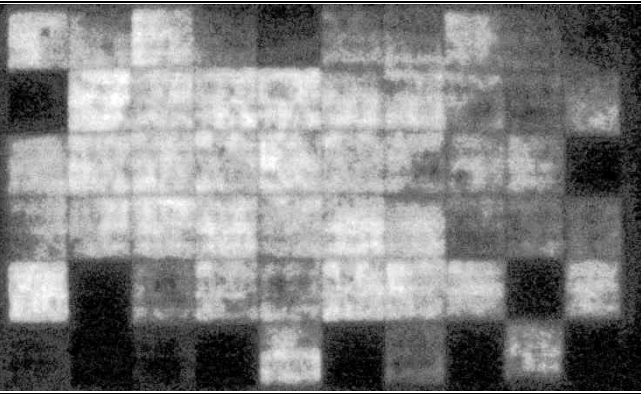

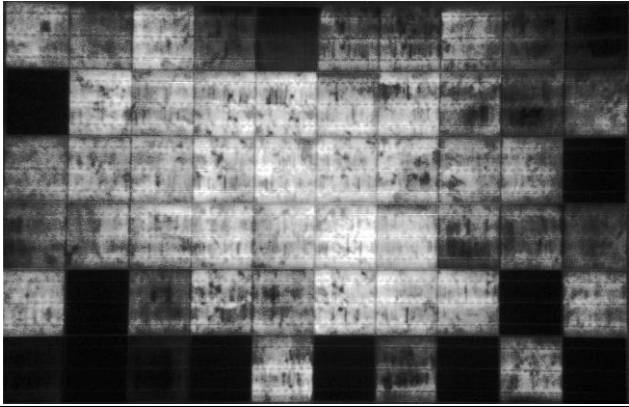

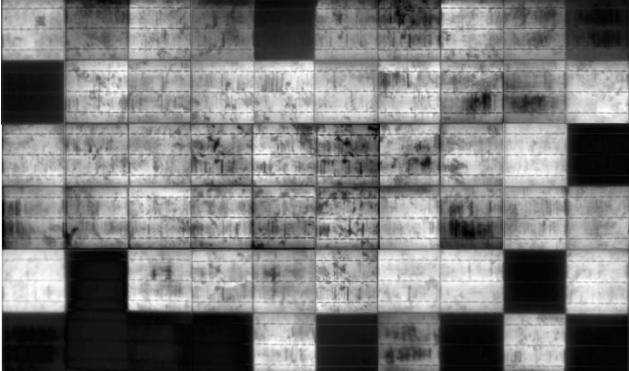


Figure 5. EL images obtained from a damaged cell with microcracks and dead fingers using 4 different cameras: (a) Sony Cyber-shot DSC-WX9, (b) GoPro HERO 3 Plus Black, (c) Canon Rebel EOS T6i and (d) Canon EOS M3.



Table 1. EL image comparison between different types of cameras.

1	<p>Sony Cyber-shot DSC-WX9</p>  <p>Price: US\$ 75.00 Modification cost: US\$ 16</p>	
2	<p>GoPro HERO 3 Plus Black</p>  <p>Price: US\$ 250.00 Modification cost: US\$ 21</p>	
3	<p>Canon Rebel EOS T6i - EF-S 18-55 IS STM</p>  <p>Price: US\$750.00 Modification cost: US\$ 21</p>	
4	<p>Canon EOS M3 - PV vision EL Lens 1.4/50</p>  <p>Price: US\$ 6,100.00</p>	

4. Results

Figure 6 shows the results obtained during the EL experiment. Modules marked in blue are modules that were blown away from the metallic structure during an extreme meteorological event that hit the region on October 16th, 2016 with 210 km/hour winds, prior to the experiment. Figure 7 presents the mapping of the two module-strings: string M and string P, with 13 and 16 modules, respectively. Modules in shades of green are closer to the positive end of each string, while modules in shades of red are closer to the negative end.

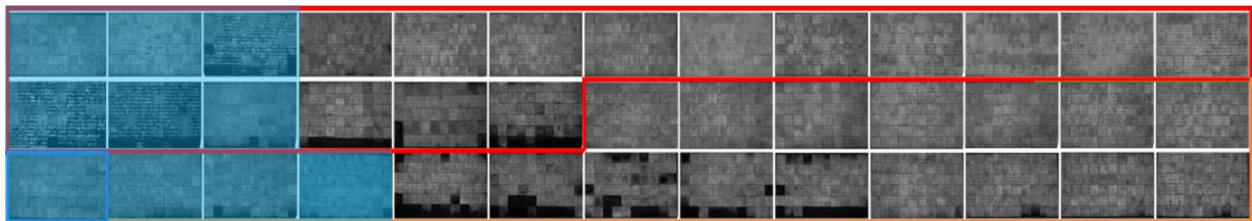


Figure 6. EL images obtained during the experiment.

M10	M9	M8	M7	M6	M5	M4	M3	M2	M1
M11	M12	M13	P1	P2	P3	P4	P5	P6	P7
	P16	P15	P14	P13	P12	P11	P10	P9	P8

Figure 7. Map of the PV module strings analysed in the study, with modules closer to the positive end of the string in green and to the negative end in red.

Modules located towards the negative end of the strings presented more darkened cells on the EL image. The evident pattern is associated with PID, and the edges are more affected because of the shorter distance of the cell to the PV module frame, which allows a shorter resistance of the path for the leakage currents between the cells and the frame (Oh et al., 2017).

Figure 8 shows the IV-curves of the P and M strings modules. The modules closest to the negative end of the string are those that present a reduction in shunt resistance, open circuit voltage and decrease of the P_{MPP} , resulting in the junction becoming less capable of separating holes and electrons (Pingel et al, 2010).

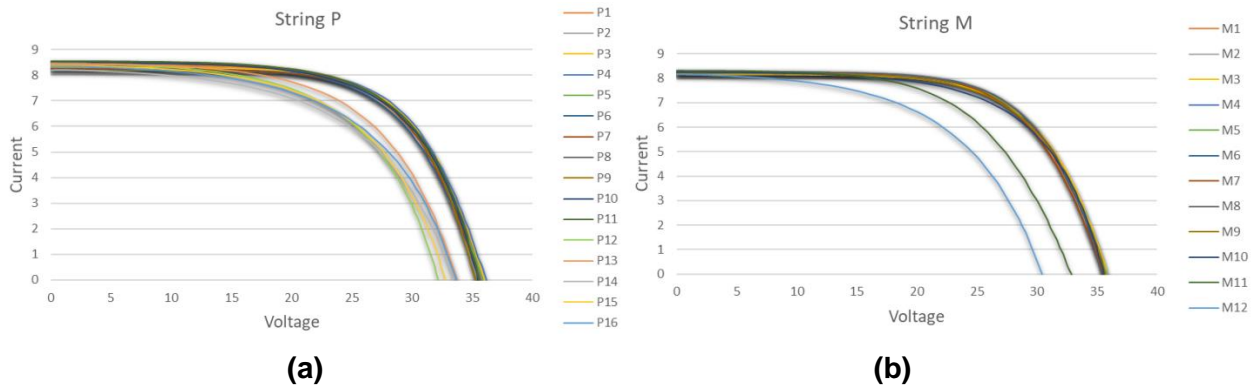


Figure 8. Individually measured IV-curves for each of the PV modules on the P and M string.

One can observe each of these parameters separately, and prove that the decrease in power due to PID occurs sequentially, that is, if shunt resistance decreases as a result, V_{OC} and P_{MPP} will also decrease (Wonwook Oh et al, 2017).

Figure 9 and Figure 10 show the decrease of the shunt resistance along the strings P and M, and the measured power and open circuit voltage relative to the “healthiest” module in the string (obtained from individually measured IV-curves), respectively.

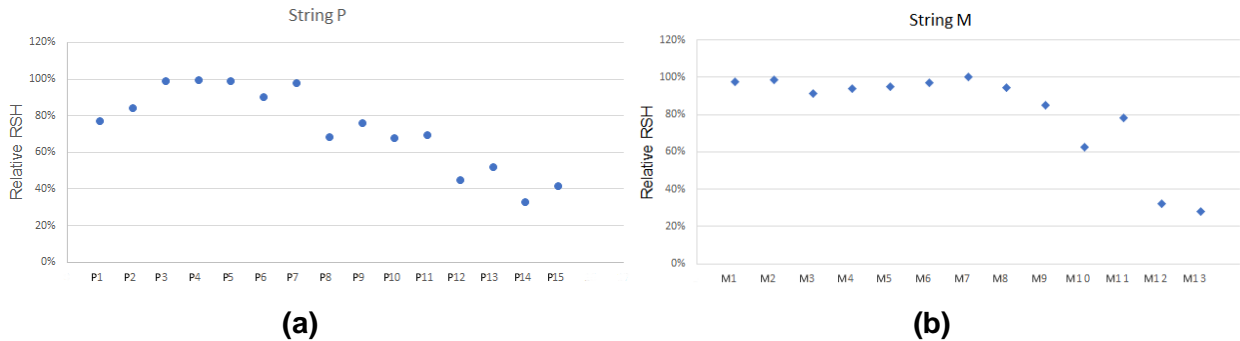


Figure 9. Decrease of the shunt resistance along strings P(a) and M(b).

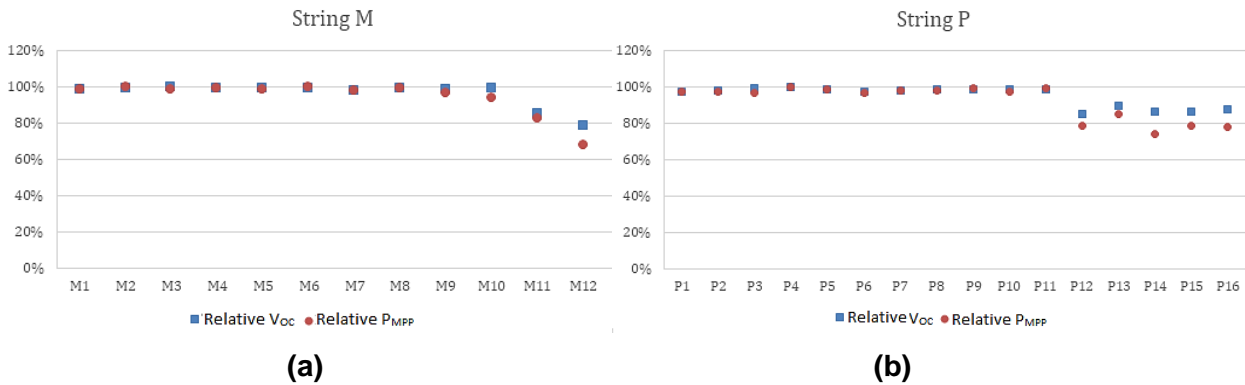


Figure 10. Measured power and open circuit voltage relative to the healthiest module in the string, obtained from individually measured IV-curves along the strings P(a) and M(b).

The images show that the degradation is more critical on the module cells closer to the negative side of the strings. These modules present a decrease in R_{SH} and V_{OC} values proportionally as the P_{MPP} also decreases. The low luminescence emission is directly associated to module efficiency losses.

5. Conclusions

In this paper, a low-cost electroluminescence technique for the detection of PID in the field was described and proven to be effective. Even with the low-resolution camera, the PID pattern was clear and easily detected. A few more expensive models of cameras could be used to improve the tests, that is, in addition to detecting totally degraded cells, could be able to perceive other types of module failures, such as microcracks and bad soldering problems, but for the specific case of PID detection, the camera chosen was the best cost-benefit.

The procedure was validated through the measurement of the module IV-curves, showing a decrease in shunt resistance, open-circuit voltage, and maximum power point.

The effectiveness of the method is relevant, as it allows the electroluminescence inspection in the field with non-expensive equipment. It also indicates the possibility of using different types of cameras, allowing their integration on devices to facilitate the inspection on site, like tripods and UAV.

References

- Colli, A., 2013, 'The role of sodium in photovoltaic devices under high voltage stress: A holistic approach to understand unsolved aspects', *Renewable Energy*, v. 60, p. 162–168.
- Djordjevic, S., Parlevliet, D., & Jennings, P., 2014, 'Detectable faults on recently installed solar modules in Western Australia. *Renewable Energy*', v. 67, p. 215–221.
- Frazão, M., Silva, J. A., Lobato, K., & Serra, J. M., 2017, 'Electroluminescence of silicon solar cells using a consumer grade digital camera', v. 99, p. 7–12.
- IEA-PVPS, 'Review on Infrared and Electroluminescence Imaging for PV Field Applications'. Report IEA-PVPS T13-10:2018
- International Renewable Energy Agency (IRENA). Available: <http://resourceirena.irena.org/gateway/dashboard/?topic=4&subTopic=16> [Accessed: 14-Jun-2018].
- Luo, W., Khoo, Y. S., Naumann, V., Lausch, D., Harvey, S. P., Ramakrishna, S., 2017, 'Potential-Induced degradation in photovoltaic modules: a critical review', *Energy Environ, Sci*, v. 10(1), p. 43–68.
- Martínez-Moreno, F., Figueiredo, G. and Lorenzo, E., 2018, 'In-the-field PID related experiences', *Solar Energy Materials and Solar Cells*, v. 174, n. September 2017, p. 485–493.
- Nascimento, L., Braga, M., Dolla, R., Campos, R. and Rüther, R., 2018, 'PV Systems in Warm and Sunny Climates: Performance Assessment of Commercially Available Solar Photovoltaic Technologies under Different Climatic Conditions in the Brazilian Energy Mix', *Photovoltaic Specialists Conference (PVSC), 45th IEEE, 2018*.
- Naumann, V., Lausch, D., Hahnel, A., Bauer, J., Breitenstein, O., Graff, A., Werner, M., Swatek, S., Grober, S., Bagdahn, J. and Hagendorf, C., 2014, 'Explanation of potential-induced degradation of the shunting type by Na decoration of stacking faults in Si solar cells', *Solar Energy Materials and Solar Cells*, v. 120, p. 383–389.



ASIA-PACIFIC
SOLAR RESEARCH
CONFERENCE

Oh, W., Bae, S., Chan, S., Lee, H., Kim, D. and Park, N., 2017, 'Field degradation prediction of potential induced degradation of the crystalline silicon photovoltaic modules based on accelerated test and climatic data', *Microelectronics Reliability*, v. 76–77, p. 596–600.

Pingel, S., Frank, O., Winkler, M., Daryan, S., Geipel, T., Hoehne, H. and Berghold, J., 2010 'Potential Induced Degradation of solar cells and panels.', *Photovoltaic Specialists Conference (PVSC), 35th IEEE, 2010. Anais.*, 2010.v.p. 002817-002822.

Rüther, R., Nascimento, L. and Campos, R., 2017, 'Performance assessment issues in utility-scale photovoltaics in warm and sunny climates', *Renew. Energy Environ. Sustain.*, v. 2, p. 35.

Acknowledgements

The authors acknowledge with thanks the Brazilian Electrical Energy Agency – ANEEL and ENGIE Brasil Energia for sponsoring the R&D project which led to the results presented in this paper.